

# Non-Darcy Permeability Parameters of Broken Rock Accompanied by Mass Loss

**Hailing Kong**

*Civil Engineering Department, Yancheng Institute of Technology, Yancheng,  
Jiangsu 224051, China*

**Luzhen Wang\***

*Civil Engineering Department, Yancheng Institute of Technology, Yancheng,  
Jiangsu 224051, China*

*\*Corresponding author*

**Xiaojian Huang, Hu Li, Haocheng Lu, Huimin Yang,  
Haipeng Xu, Zhen Xue**

*Civil Engineering Department, Yancheng Institute of Technology, Yancheng,  
Jiangsu 224051, China*

## ABSTRACT

Permeability tests of broken rock accompanying by mass loss were carried out by the self-designed pump-type permeability testing system, in which samples were divided into 10 Talbol power exponents and 5 compression. The permeability parameters of broken rock accompanying by mass loss, including permeability, non-Darcy flow  $\beta$  factor and acceleration coefficient, were calculated by a genetic algorithm. Combining the test phenomena, theoretical analysis and numerical calculation, the varying laws of non-Darcy permeability parameters of broken rock accompanying by mass loss were obtained. It shows that, (1) the varying laws of non-Darcy permeability parameters have characteristics of nonlinear time-varied, and the varying curves are divided into three stages, the initial seepage, the upheaval seepage and the slowly-changing seepage. (2) With the increasing of test time, permeability increases, while non-Darcy flow  $\beta$  factor and acceleration coefficient decrease, respectively. (3) The magnitudes of permeability parameters steps down with the increasing of Talbol power exponent and compression. Samples above the step have obvious upheaval seepage, and seepage is unstable. (4) The sample with a Talbol power exponent of 0.1 and a compression of 0 has seepage much closer to the Darcy flow. This study provides theoretical and experimental basis for researching the mechanism of seepage instability of broken rock accompanying by mass loss.

**KEYWORDS:** mass loss; broken rock; non-Darcy seepage; permeability parameters.

## INTRODUCTION

Surrounding structure always destroyed and fractured into broken rock during construction in geotechnical engineering, for instance, mining and tunneling. The broken surrounding rock has several natural water flowing channels, which brings a lot of hidden trouble to engineering's construction and business. Due to the effect of corrosion, abrasion and erosion, fine particles in the broken surrounding rock migrate with water in the seepage process. It is the migration and mass loss of fine particles that result in the characteristics of nonlinear time-varied of pore structure and permeability parameters (including permeability, non-Darcy flow  $\beta$  factor and acceleration coefficient) consequentially. When the permeability parameters in the broken surrounding rock change to a certain extent, the seepage system mutates because of structural instability<sup>[1-3]</sup>, and the water flow type also varies from seepage to pipe flow<sup>[4]</sup>. Therefore, it is very important in engineering practice to study the varying laws of the migration and permeability parameters of broken rock for researching the nonlinear time-varied seepage behavior and the disasters caused by seepage instability.

So far, the research methods of permeability parameters of broken rock with constant quality can be summarized as two categories, load control method and porosity control method. The former is used to test permeability parameters at different seepage velocities when axial load is constant, while the latter is used to test permeability parameters at different seepage velocities when the porosity is constant. Permeability and non-Darcy flow  $\beta$  factor obey the Forchheimer law, and could be gained by the method of least squares nonlinear regression<sup>[5]</sup>. Sun et al. studied seepage characteristics of broken sandstone with 4 grain sizes, and gained the relations between seepage characteristics and load or grain size by the two element-nine parameter regression method. Liu, Ma, et al.<sup>[7-9]</sup> tested permeability of broken sandstone and coal with different grain sizes at different axial stresses, drawn curves between permeability coefficient and time or axial stress, regressed the functions between permeability coefficient  $K$  and axial stresses. Huang et al.<sup>[10]</sup> found that the relations between porosity and permeability or non-Darcy flow  $\beta$  factor could be fitted by power functions, and considered that seepage characteristics of broken rock were relative with loading history. Li et al.<sup>[11]</sup> studied seepage characteristics of broken sandstone, gangues and limestone with single grain size and distributed grain sizes. Wang, Kong, Chen, et al.<sup>[12-13]</sup> tested permeability of broken gangues and coal, and obtained relations between permeability parameters and loading history or loading type or porosity.

To sum up, researches on permeability parameters of broken rock with constant quality is already quite mature, however, academic researches are insufficient for permeability parameters of broken rock accompanying by mass loss. Because seepage of broken rock has nonlinear character, seepage system has more significant nonlinear behavior and time varying character when considering mass loss, and it is difficult to regress permeability parameter containing acceleration coefficient by traditional least square method. So that, it is of difficulty to research the varying laws of permeability parameters of broken rock accompanying by mass loss.

In this paper, the nonlinear time-varied characteristics of permeability parameters of broken rock resulting from mass loss was raised with genetic algorithm and calculated by Fortran response programs. More concretely, we tested permeability parameters of broken rock accompanying by mass loss by the self-made permeation test device, calculated the time series of permeability parameters by collecting data of flow and permeable pressure, studied the influence on permeability parameters of grain sizes and density of broken rock in the surrounding rock, and analyzed the varying laws of permeability parameters affected by Talbol power exponents and compression. Results in this paper will provide theoretical and experimental basis for further research on the seepage instability mechanism of broken rock in geotechnical engineering.

## TESTING SYSTEM AND METHOD

### Testing System

The seepage testing system for broken rock accompanying by mass loss is mainly constituted by the permeation test system and the material testing machine, as shown in Fig. 1, the former is constituted by permeameter, the quantitative plunger pump, spill valves, reversal valve, flow transducer, pressure transducer, vibrating screen, water tank, and so on.

Sample is placed in the permeameter, and loaded by the material testing machine. Water is pumped from tank by the plunger pump, flowed into the bottom of the permeameter through reversing valve, flow sensors and pressure sensors, permeated samples. In this test process, permeable pressure difference is controlled by the relief valve, and water flow and pressure at the bottom of samples are collected by flow sensors and pressure sensors, respectively. The lost mass spurts out of the permeameter accompanying with water, converges at the tray, and flows into the vibrosieve through hose.

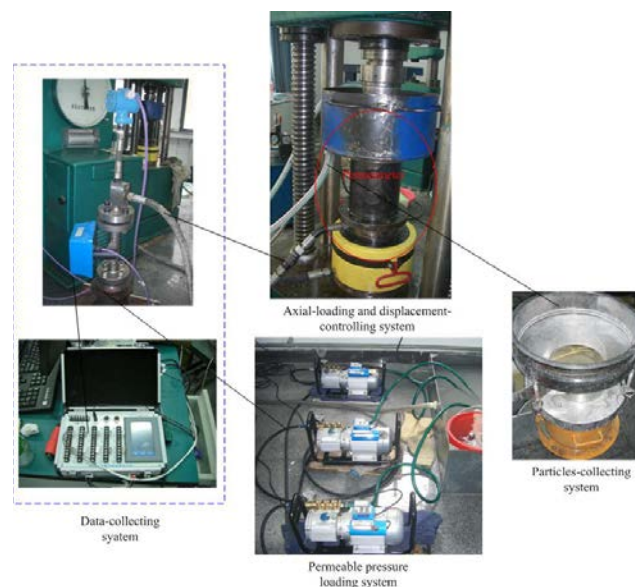


Fig.1 Test system

## Testing Method

In this paper, the influence on permeability parameters of grain size and density of broken rock are considered comprehensively. Mudstone is used as samples in this test, which is broken into 8 kinds of grain sizes. Samples are matched by the Talbol continuous grading formula<sup>[15-16]</sup>, and the Talbol power exponents are set as 0.1, 0.2, ... 0.9, and 1.0, respectively. Considering the influence of the density of broken rock, samples are compressed 0 mm, 10 mm, 20 mm, 30 mm or 40 mm, respectively. Tests under 10 different Talbol power exponents and 5 different compression degrees are carried out, and in order to obtain more effective data, the duration of each test is larger than 18000 s.

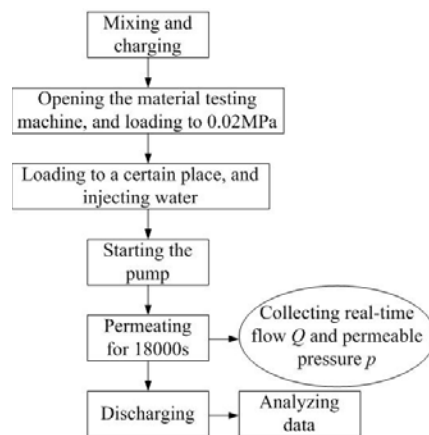


Fig. 2 The flow diagram of the test

The testing process is divided into the following main steps: mixing and charging, loading, water injecting, permeating, data collecting and discharging, as shown in Fig. 2.

## CALCULATING METHOD FOR PERMEABILITY PARAMETERS OF BROKEN ROCK ACCOMPANYING BY MASS LOSS

Broken rock in geotechnical engineering is mainly composed of particles with different grain sizes, so it is inaccurate to calculate the permeability at every sampling time by the Darcy's Law<sup>[17]</sup>. Due to the fine particles' migration and mass loss in the seepage process of broken rock, the seepage could not reach the steady state if the pressure gradient is larger and the flow velocity is faster, then seepage obeys the Forchheimer momentum equation.

The gravity of the particles is negligible, because the grain size of the migrated particles are so little that their gravity are much lower than the action from water pressure. In this test, water flows from the water inlet pipe at the bottom of the permeameter into the cavity, permeates through broken rock and flows out from the piston bore, so that its flowing process could be approximated as an kind of bottom-up unidirectional flow, which could be simplified as one dimensional single phase non-Darcy flow, and expressed by the Forchheimer momentum equation as follow:

$$\rho_l c_a \frac{\partial V}{\partial t} = -\frac{\partial p}{\partial x} - \frac{\mu_0}{k} V - \rho_l \beta V^2 \quad (1)$$

Where,  $\rho_l$  is the mass density of fluid;  $c_a$  is acceleration coefficient;  $V$  is seepage velocity, which is calculated by the flow  $Q$ , that is  $V = \frac{Q}{\pi a^2}$ ;  $p$  is permeable pressure;  $x$  is the coordinate in the vertical direction of the sample;  $k$  is the non-Darcy flow permeability;  $\mu_0$  is dynamic viscosity of liquid and  $\beta$  is non-Darcy flow  $\beta$  factor.

Power exponent relations are existed between porosity and permeability or non-Darcy flow  $\beta$  factor or acceleration coefficient, which are listed as follows

$$k_i = k_r \left( \frac{\varphi}{\varphi_r} \right)^{m_k} \quad \beta_i = \beta_r \left( \frac{\varphi}{\varphi_r} \right)^{m_\beta} \quad c_a^i = c_{ar} \left( \frac{\varphi}{\varphi_r} \right)^{m_{c_a}} \quad (2)$$

where  $\varphi_r$  was the reference value of porosity,  $k_r$  was permeability corresponding to the reference value of porosity,  $\beta_r$  was non-Darcy flow  $\beta$  factor corresponding to the reference value of porosity,  $c_{ar}$  was acceleration coefficient corresponding to the reference value of porosity, and the power exponents  $m_k$ ,  $m_\beta$  and  $m_{c_a}$  were measured by tests, which were related to lithology, initial porosity, Talbol power exponent, and so on.

The response program are coded by Fortran in two steps:

Firstly, algebraic equations of permeability at each sampling time are established based on the power relations and Forchheimer momentum equation among permeability parameters of broken rock, and the roots of algebraic equations are calculated by Newton tangent method<sup>[18]</sup>.

Secondly, according to the genetic algorithm, the reference values and power exponents of permeability parameters are optimized in four steps<sup>[19]</sup>: a. using three node interpolation to deal with permeability parameters in whole range; b. calculating numerical solution of the momentum equation by Runge-Kutta method with variable step; c. judging whether the error between numerical solution of the seepage velocity and the testing result meets the requirement or not; d. if the error could not

meet the requirement, readjusting the reference values and power exponents of permeability parameters until the requirements were met.

According to the collected flow and permeable pressure at sampling time during the process of seepage test, seepage velocity and pressure gradient at sampling time can be calculated easily, then permeability parameters of the non-Darcy flow of broken rock at sampling time also can be calculated by the formula (3).

$$\rho c_a^i a_i = -G_i - \frac{\mu}{k_i} V_i - \rho \beta_i V_i^2, \quad i=0,1,2,\dots,N \quad (3)$$

## TESTING RESULTS AND ANALYSIS

### Time-Varying Laws of Permeability Parameters Influenced by Talbol Power Exponents and Compression

The characteristics of the time-varying laws of permeability parameters are related with the upheaval seepage, which is influenced by Talbol power exponents and compression of samples directly.

**Table 1:** The change of magnitudes of permeability in the whole test

Talbol power exponents	Magnitudes of permeability under different compression(m <sup>2</sup> )				
	0mm	10mm	20mm	30mm	40mm
0.1	10 <sup>-14</sup> ~10 <sup>-10</sup>	10 <sup>-14</sup> ~10 <sup>-11</sup>			
0.2	10 <sup>-12</sup> ~10 <sup>-11</sup>	10 <sup>-14</sup> ~10 <sup>-11</sup>	10 <sup>-14</sup> ~10 <sup>-11</sup>	10 <sup>-14</sup> ~10 <sup>-11</sup>	10 <sup>-14</sup> ~10 <sup>-11</sup>
0.3	10 <sup>-12</sup> ~10 <sup>-11</sup>	10 <sup>-14</sup> ~10 <sup>-11</sup>	10 <sup>-14</sup> ~10 <sup>-11</sup>	10 <sup>-14</sup> ~10 <sup>-11</sup>	10 <sup>-14</sup> ~10 <sup>-11</sup>
0.4	10 <sup>-12</sup> ~10 <sup>-11</sup>	10 <sup>-12</sup> ~10 <sup>-11</sup>	10 <sup>-14</sup> ~10 <sup>-11</sup>	10 <sup>-14</sup> ~10 <sup>-11</sup>	10 <sup>-14</sup> ~10 <sup>-11</sup>
0.5	10 <sup>-12</sup> ~10 <sup>-11</sup>	10 <sup>-12</sup> ~10 <sup>-11</sup>	10 <sup>-14</sup> ~10 <sup>-11</sup>	10 <sup>-14</sup> ~10 <sup>-11</sup>	10 <sup>-14</sup> ~10 <sup>-11</sup>
0.6	10 <sup>-12</sup> ~10 <sup>-11</sup>	10 <sup>-12</sup> ~10 <sup>-11</sup>	10 <sup>-14</sup> ~10 <sup>-11</sup>	10 <sup>-14</sup> ~10 <sup>-11</sup>	10 <sup>-14</sup> ~10 <sup>-11</sup>
0.7	10 <sup>-12</sup> ~10 <sup>-11</sup>	10 <sup>-12</sup> ~10 <sup>-11</sup>	10 <sup>-12</sup> ~10 <sup>-11</sup>	10 <sup>-12</sup> ~10 <sup>-11</sup>	10 <sup>-14</sup> ~10 <sup>-11</sup>
0.8	10 <sup>-11</sup> ~10 <sup>-11</sup>	10 <sup>-11</sup> ~10 <sup>-11</sup>	10 <sup>-12</sup> ~10 <sup>-12</sup>	10 <sup>-12</sup> ~10 <sup>-12</sup>	10 <sup>-13</sup> ~10 <sup>-11</sup>
0.9	10 <sup>-12</sup> ~10 <sup>-12</sup>	10 <sup>-12</sup> ~10 <sup>-12</sup>	10 <sup>-12</sup> ~10 <sup>-11</sup>	10 <sup>-12</sup> ~10 <sup>-11</sup>	10 <sup>-12</sup> ~10 <sup>-11</sup>

					11
1.0	$10^{-12} \sim 10^{-12}$	$10^{-12} \sim 10^{-12}$	$10^{-11} \sim 10^{-10}$	$10^{-11} \sim 10^{-10}$	$10^{-12} \sim 10^{-11}$

Table 1 gives the change of magnitudes of permeability of samples with 10 Talbol power exponents and 5 compression in the whole seepage process. It could be found that, the magnitudes of permeability steps down with the increase of Talbol power exponents and compression. These upper-right samples which have upheaval seepage stage have large difference of permeability in their initial seepage stage and the slowly-changing seepage stage, and the magnitudes of permeability upheaval from  $10^{-14} \text{ m}^2$  to  $10^{-11} \text{ m}^2$  or even  $10^{-10} \text{ m}^2$ . While those lower-left samples which do not have upheaval seepage stage have little difference of permeability in their initial seepage stage and the slowly-changing seepage stage, and permeability changes even in the same magnitude. However, no matter what kinds of samples nearly have the permeability with the constant magnitude in their slowly-changing seepage stage.

**Table 2:** The change of magnitudes of non-Darcy flow  $\beta$  factor in the whole test

Talbol power exponents	Magnitudes of non-Darcy flow $\beta$ factor under different compression( $\text{m}^{-1}$ )				
	0mm	10mm	20mm	30mm	40mm
0.1	$10^{11} \sim 10^3$	$10^{11} \sim 10^5$	$10^{11} \sim 10^5$	$10^{11} \sim 10^6$	$10^{12} \sim 10^6$
0.2	$10^7 \sim 10^5$	$10^{11} \sim 10^5$	$10^{11} \sim 10^5$	$10^{10} \sim 10^5$	$10^{12} \sim 10^5$
0.3	$10^9 \sim 10^4$	$10^{11} \sim 10^5$	$10^{11} \sim 10^4$	$10^{11} \sim 10^5$	$10^{12} \sim 10^5$
0.4	$10^8 \sim 10^5$	$10^8 \sim 10^5$	$10^{11} \sim 10^4$	$10^{11} \sim 10^5$	$10^{12} \sim 10^5$
0.5	$10^7 \sim 10^6$	$10^{11} \sim 10^4$	$10^{11} \sim 10^5$	$10^9 \sim 10^4$	$10^{11} \sim 10^5$
0.6	$10^7 \sim 10^6$	$10^8 \sim 10^6$	$10^{11} \sim 10^5$	$10^{11} \sim 10^5$	$10^9 \sim 10^5$
0.7	$10^7 \sim 10^6$	$10^9 \sim 10^5$	$10^{10} \sim 10^6$	$10^8 \sim 10^8$	$10^{11} \sim 10^7$
0.8	$10^6 \sim 10^6$	$10^6 \sim 10^6$	$10^7 \sim 10^6$	$10^8 \sim 10^8$	$10^9 \sim 10^6$
0.9	$10^8 \sim 10^7$	$10^7 \sim 10^7$	$10^8 \sim 10^5$	$10^8 \sim 10^6$	$10^8 \sim 10^8$
1.0	$10^7 \sim 10^7$	$10^7 \sim 10^7$	$10^7 \sim 10^6$	$10^4 \sim 10^4$	$10^7 \sim 10^7$

Table 2 gives the change of magnitudes of non-Darcy flow  $\beta$  factor of samples with 10 Talbol power exponents and 5 compression in the whole seepage process.

Obviously, the magnitudes of non-Darcy flow  $\beta$  factor also steps down with the increase of Talbol power exponents and compression. The magnitudes of non-Darcy flow  $\beta$  factor of the sample with a Talbol power exponent of 0.1 and a compression of 0 have the biggest drop after the upheaval seepage stage, and the magnitudes are as lower as  $10^3 \text{ m}^{-1}$ , which is related with the type of seepage channels of this sample after the upheaval seepage stage. It has high content of fine particles which are easy to migrate with water flow in the sample with a Talbol power exponent of 0.1, this sample is just heaped up by loose sand when its compression is 0, and sieve-like seepage channels will form rapidly inside this sample under the permeable pressure. The seepage type is close to Darcy flow but not the non-Darcy flow, under the circumstances.

Tab.3 The change of magnitudes of acceleration coefficient in the whole test

Talbol power exponents	Magnitudes of acceleration coefficient under different compression				
	0mm	10mm	20mm	30mm	40mm
0.1	$10^9 \sim 10^4$	$10^{10} \sim 10^6$	$10^{11} \sim 10^6$	$10^{11} \sim 10^6$	$10^{11} \sim 10^6$
0.2	$10^7 \sim 10^6$	$10^{10} \sim 10^6$	$10^{10} \sim 10^6$	$10^{10} \sim 10^6$	$10^{11} \sim 10^6$
0.3	$10^7 \sim 10^5$	$10^{10} \sim 10^6$	$10^{11} \sim 10^5$	$10^{11} \sim 10^6$	$10^{11} \sim 10^6$
0.4	$10^8 \sim 10^6$	$10^8 \sim 10^6$	$10^{10} \sim 10^5$	$10^{10} \sim 10^6$	$10^{11} \sim 10^6$
0.5	$10^7 \sim 10^6$	$10^8 \sim 10^5$	$10^{10} \sim 10^6$	$10^{10} \sim 10^5$	$10^{11} \sim 10^6$
0.6	$10^8 \sim 10^6$	$10^8 \sim 10^7$	$10^{10} \sim 10^6$	$10^{10} \sim 10^6$	$10^{10} \sim 10^6$
0.7	$10^7 \sim 10^7$	$10^8 \sim 10^6$	$10^9 \sim 10^6$	$10^8 \sim 10^8$	$10^{11} \sim 10^7$
0.8	$10^7 \sim 10^7$	$10^7 \sim 10^7$	$10^7 \sim 10^7$	$10^8 \sim 10^8$	$10^9 \sim 10^7$
0.9	$10^8 \sim 10^7$	$10^7 \sim 10^7$	$10^8 \sim 10^6$	$10^8 \sim 10^7$	$10^8 \sim 10^8$
1.0	$10^7 \sim 10^7$	$10^7 \sim 10^7$	$10^7 \sim 10^7$	$10^5 \sim 10^5$	$10^7 \sim 10^7$

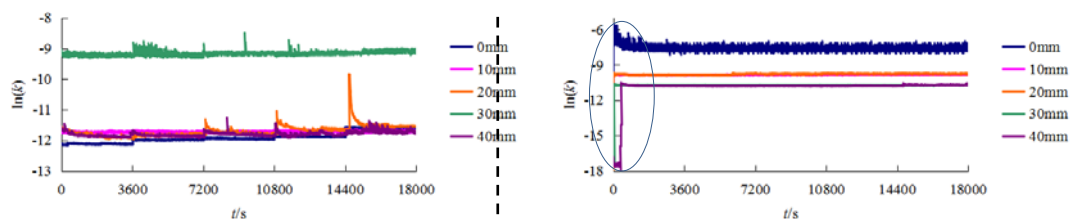
Table 3 gives the change of magnitudes of acceleration coefficient of samples with 10 Talbol power exponents and 5 compression in the whole seepage process. Just as the varying law of permeability and non-Darcy flow  $\beta$  factor, the magnitudes of acceleration coefficient also steps down with the increase of Talbol power exponents and compression.

The magnitudes of acceleration coefficient of the sample with a Talbol power exponent of 0.1 and a compression of 0 also have the biggest drop after the upheaval seepage stage, and the magnitudes are as lower as  $10^4$ .

As shown in Tab.1, Tab.2 and Tab.3, the upper-right samples have obvious upheaval seepage stage, because the magnitudes of permeability, non-Darcy flow  $\beta$  factor and acceleration coefficient varied in a wide range, and seepage in these samples are unstable seepage. While the lower-left samples' magnitudes of permeability, non-Darcy flow  $\beta$  factor and acceleration coefficient vary smaller and smaller with the increase of Talbol power exponents and the decrease of compression, and seepage in those sample are very stable.

### The Comparison of Time-Varying Laws of Permeability Parameters between Samples

In this paper, samples with obvious upheaval seepage or with stable seepage all be mentioned above, but the details of their differences haven't introduced yet.



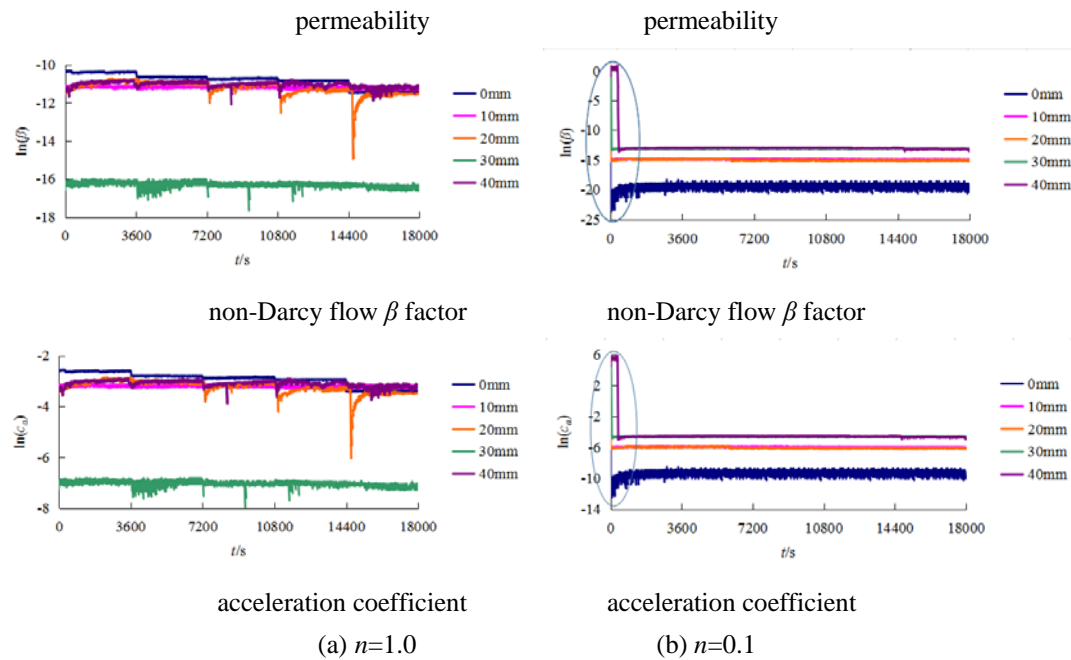


**Figure 3:** The comparison of time-varying laws of permeability parameters between samples

Figure 3 shows the comparison of time-varying laws of permeability parameters between samples with Talbol power exponents of 1.0 and 0.1. Thereinto, the left list is 1.0 and the right list is 0.1.

As shown in the left list of Fig. 3, permeability parameters of sample with Talbol power exponents of 1.0 vary a little besides the curve of compression of 20mm, which corroborates that seepage in the lower-left samples are stable. The reason why the curve of compression of 20mm has larger change is that the pumps in our test system has some problem with its water inlets, so that the permeameter is lack of water, which causes the phenomenon of the larger changes in the curve of compression of 20mm.

It can be found in the right list of Fig. 3 that permeability parameters of sample with Talbol power exponents of 0.1 upheaval a lot, which shows that seepage in the upper-right samples always have upheaval seepage stage. The upheaval seepage stage often occurs at the very beginning of the seepage process, which is rounded in the right part of Fig.3.

## CONCLUSIONS

In this paper, seepage tests of broken rock accompanying by mass loss are carried out based on the self-designed pump-type permeability testing system, and samples are distributed into 10 Talbol power exponents and 5 compression. The permeability parameters, including permeability, non-Darcy flow  $\beta$  factor and acceleration coefficient, are calculated by the genetic algorithm. The varying laws of non-Darcy permeability parameters of broken rock accompanying by mass loss are obtained

comprehensively considering the test phenomena, theoretical analysis and numerical calculation. Conclusions are listed as follows:

The varying laws of non-Darcy permeability parameters have characteristics of nonlinear time-varied. The varying curves are divided into three stages, the initial seepage, the upheaval seepage and the slowly-changing seepage.

With the increasing of test time, permeability of broken rock increases, while non-Darcy flow  $\beta$  factor and acceleration coefficient decrease, and the varying ranges of permeability parameters are closely related with Talbol power exponents and compression.

The magnitudes of permeability parameters steps down with the increasing of Talbol power exponent and compression.

The upper-right samples have obvious upheaval seepage stage, and seepage is unstable. While the lower-left samples' magnitudes of permeability parameters vary smaller and smaller with the increase of Talbol power exponents and the decrease of compression, and seepage is very stable.

The sample with a Talbol power exponent of 0.1 and a compression of 0 has seepage much closer to the Darcy flow.

Seepage in the lower-left samples are stable, while seepage in the upper-right samples always have upheaval seepage stage, and the upheaval seepage stage often occurs at the very beginning of the seepage process.

## ACKNOWLEDGEMENTS

Project supported by the National Natural Science Fund (11502229), the Natural Science Foundation of Jiangsu Province of China (BK20160433), the Outstanding Young Backbone Teacher of Qinglan Project in Jiangsu Province, the Program of Outstanding Young Scholars in Yancheng Institute of Technology, Jiangsu College students' innovation entrepreneurship training program (201610305040Y) and the opening foundation of laboratory in Yancheng Institute of Technology.

## REFERENCES

1. Li, S. C, Miao, X. X, Chen, Z. Q, (2005), "Nonlinear dynamic analysis on non-Darcy seepage in over-broken rock mass." *Journal of China Coal Society*, Vol. 30(5), pp. 557-561.
2. Miao, X. X, Li, S. C, Chen, Z. Q, (2009), "Bifurcation and catastrophe of seepage flow system in broken rock." *Mining Science and Technology*, Vol. 19(1), pp. 1-7.
3. Kong, H. L, Miao, X. X, Wang, L. Z, Zhang, Y, Chen, Z. Q, (2007), "Analysis of the harmfulness of water-inrush from coal seam floor based on seepage instability theory."

- Mining Science and Technology (Journal of China University of Mining and Technology (English Edition) ), Vol. 17(4), pp. 453-458.
4. Wang, L. Z, Chen, Z. Q, Shen H. D, (2013), "Experimental study on the type change of liquid flow in broken coal." *Journal of Coal Science and Engineering (China)*, Vol. 19(1), pp. 19-25.
  5. Miao, X. X, Li, S. C, Chen, Z. Q, Liu, W. Q, (2011), "Experimental study of seepage properties of broken sandstone under different porosities." *Transport in Porous Media*, Vol. 86(3), pp. 805-814.
  6. Sun, M. G, Li, T. Z, Huang, X. W, Chen, R. H, (2003), "Penetrating properties of non-Darcy flow in fragmentized rocks." *Journal of Anhui University of Science and Technology (Natural Science)*, Vol. 23(2), pp. 11-13.
  7. Liu, W. Q, Miao, X. X, Chen, Z. Q, (2003), "A testing method for determining the permeability of overbroken rock." *Journal of Experimental Mechanics*, Vol. 18(1), pp. 57-61.
  8. Ma, Z. G, Miao, X. X, Li, X. H, Guo, G. L, Shi, X. S, (2007), "Permeability of broken shale." *Journal of Mining & Safety Engineering*, Vol. 24(3), 260-264.
  9. Ma, Z. G, Miao, X. X, Zhang, F, Li, Y. S, (2007), "Experimental Study into Permeability of Broken Mudstone." *Journal of China University of Mining & Technology*, Vol. 17(2), pp. 147-151.
  10. Huang, X. W, Tang, P, Miao, X. X, Chen, Z. Q, (2005), "Testing study on seepage properties of broken sandstone." *Rock and Soil Mechanics*, Vol. 26(9), pp. 1385-1388.
  11. Li, S. C, Miao, X. X, Chen, Z. Q, Mao, X. B, (2008), "Experimental study on seepage properties of non-Darcy flow in confined broken rocks." *Engineering Mechanics*, Vol. 25(4), pp. 85-92.
  12. Wang, L. Z, Chen, Z. Q, Kong, H. L, Shen H. D, (2013), "Experimental study of impact of loading history on permeability characteristics of broken coal with different particle size gradations." *Rock and Soil Mechanics*, Vol. 34(5), pp. 1325-1330.
  13. Kong, H. L, Chen, Z. Q, Wang, L. Z, Shen, H. D, (2013), "Experimental study on permeability of crushed gangues during compaction." *International Journal of Mineral Processing*, Vol. 124, pp. 95-101.
  14. Wang, L. Z, Wang, B, Chen, Z. Q, Kong, H. L, (2014), "The rule of mass loss for broken mudstone under scouring effect." *Electronic Journal of Geotechnical Engineering*, Vol. 19(V), pp. 8705-8715.
  15. Wang, L. Z, Chen, Z. Q, Kong, H. L, (2014), "Influences on penetration laws of broken mudstone with mass loss from Talbol power exponents." *Electronic Journal of Geotechnical Engineering*, Vol. 19(O), pp. 3681-3692.

16. Wang, L. Z, Kong, H. L, Wang, W, Hui, W. R, Wang, Z. Y, (2015), "Experimental study on the fractal feature of confined broken gangues." *Electronic Journal of Geotechnical Engineering*, Vol. 20(21), pp. 12047-12056.
17. Yao, B. H, (2012), "Research on variable mass fluid-solid coupling dynamic theory of broken rock mass and application." China University of Mining & Technology.
18. Chen, Z. Q, Wang, L. Z, Kong, H. L, Ni, X. Y, Yao, B. H, (2014), "A method for calculating permeability parameters of variable mass of broken rock." *Chinese Journal of Applied Mechanics*, Vol. 19(O), pp. 3681-3692.
19. Chen, Z. Q, Feng, M. M, Wang, L. Z, Zhu, N. J, Ni, X. Y, Zhang, G. Y, Zhou, M, Wang, Z. F, (2014), "A calculating method for permeability parameters of variable mass of broken rock." ( a published patent )



© 2017 ejge

***Editor's note.***

This paper may be referred to, in other articles, as:

Hailing Kong, Luzhen Wang, Xiaojian Huang, Hu Li, Haocheng Lu, Huimin Yang, Haipeng Xu, and Zhen Xue: "Non-Darcy Permeability Parameters of Broken Rock Accompanied by Mass Loss" *Electronic Journal of Geotechnical Engineering*, 2017 (22.01), pp 119-130. Available at [ejge.com](http://ejge.com).